Received: 27 February 2021 | Revised: 25 June 2021 | Accepted: 29 July 2021

DOI: 10.1002/jbm.a.37292

ORIGINAL ARTICLE

Comparing the wound healing effect of a controlled release wound dressing containing curcumin/ciprofloxacin and simvastatin/ciprofloxacin in a rat model: A preclinical study

Parisa Heydari[1] | Anosheh Zargar Kharazi[1,2] | Seddigheh Asgary[3] | Shokoh Parham[1]

[1]Biomaterials Nanotechnology and Tissue Engineering Faculty, School of Advanced Technologies in Medicine, Isfahan University of Medical Sciences, Isfahan, Iran

[2]Applied physiology research center, Isfahan university of medical sciences, Isfahan, Iran

[3]Isfahan Cardiovascular Research Center, Cardiovascular Research institute, Isfahan University of Medical Sciences, Isfahan, Iran

Correspondence
Anosheh Zargar Kharazi, Biomaterials Nanotechnology and Tissue Engineering Faculty, School of Advanced, Medical Technology, Isfahan University of Medical Sciences, Isfahan, Iran.
Email: a_zargar@med.mui.ac.ir

Seddigheh Asgary, Department of Pharmacognosy Isfahan Cardiovascular Research Center, Isfahan University of Medical Sciences, Isfahan, Iran.
Email: sedighehasgary@gmail.com

Funding information
National Institute for Medical Research Development, Grant/Award Number: 963505

Abstract

Inflammation and infection are two main factors predisposing a wound to become a chronic one. Degradable wound dressings involving the controlled release of suitable drugs at the ulcer site are one of the solutions to make wounds healing progress smoothly and rapidly. In this research, biodegradable dressings made of polyglycerol sebacate/polycaprolactone (PGS/PCL) containing curcumin/ciprofloxacin (CUR/CIP) and simvastatin/ciprofloxacin (SIM/CIP) were prepared by using the coaxial electrospinning method. Transmission electron microscopy for uniform core/shell structure, swelling ratio, and drug release pattern of the wound dressings were evaluated. At the in vivo study, histometric, histopathologic, and collagen expression study was performed. The PGS/PCL samples containing SIM/CIP showed a burst release pattern of CIP with a delay in the release of SIM; meanwhile, in the samples containing CUR/CIP, both drugs showed a burst release behavior. No cytotoxicity response was observed in the study groups. The in vivo study showed that wound closure was almost completed only in the SIM/CIP group after 14 days. After 14 days, in the wound treated with SIM/CIP dressing, the amount of collagen deposition and angiogenesis was higher than that of the others. These results clearly showed the effect of SIM/CIP on the improvement of the wound healing efficiency in the long term (14 days) and the effect of CUR/CIP on wound contraction in the short term (4 day). It seems, therefore, that the use of SIM and CUR simultaneously in a wound dressing could cause a synergistic effect in the wound repair.

KEYWORDS
antibacterial, anti-inflammatory, drug delivery, polycaprolactone, polyglycerol sebacate, wound healing

1 | INTRODUCTION

Generally, the largest organ of the human body is the skin tissue. Skin is the first defense barrier of the human body against pathogenic, physical, chemical, and mechanical assaults. Therefore, it is regularly subjected to several damages including trauma, burns, chronic ulcers, and diabetic ulcers; also, the effects of sunlight are more on the skin than other human organs.[1,2] According to the report developed by the World Health Organization, 300,000 people die from burn injuries annually.[3] In the last decade, one of the common methods used to treat the burn and diabetic wounds is the autograft method. This technique has many drawbacks, such as extended treatment periods, increased treatment costs, aggravated inflammation, and, in some cases, damage to other parts of the human body.[4] Another method to treat the burn wounds is to use silver wound dressing. These wound dressings generate reactive oxygen species (ROS). ROS free radical is

more toxic to the human skin cells, thus causing delay in the healing wound process.[1]

Recently, some natural polymers such as chitosan, collagen, cellulous, gelatin, and hydrogel have been used to fabricate wound dressings. In other research studies, synthetic polymers such as polylactic acid, polyglycolic acid, and the combination of natural and synthesis polymer have been used to fabricate the ideal wound dressing.[5-7] However, this research is still in progress to achieve the ideal and suitable wound dressing.[8] Nowadays, new approaches such as the electrospinning technique have been used for the design and fabrication of biological wound dressings.[9]

Electrospinning process has shown some advantages. One is tunable porosity and the other one is that it can mimic the extracellular matrix of the skin and ensure a high surface-to-volume ratio; therefore, it can lead to cytocompatibility, with a strong ability for absorbing the microenvironment moisture and the exudates from the wound. This process produces fibers with an appropriate diameter by using an electric field and a polymer solution.[10] The most important parameters of this process are the suitable polymer, an appropriate solvent, and good environmental conditions for fabricating the ideal membranes and skin wound dressing.[11]

The core–shell system is one of the important electrospinning techniques.[12] This method, using electrospinning materials with encapsulating different drugs, can generate a nanofiber with two parts in one structure. These two are the inner (core) and outer (shell) parts. The core–shell method has demonstrated the unique platform of biomaterials for use in tissue engineering and drug delivery.[13] On the other hand, the porous structure can provide a potential morphology for using wound dressing with drug delivery at the same time. Additionally, polymers used to fabricate wound dressings should have some abilities. The first one is that they can be loaded, releasing the drugs in a controlled behavior; the other one is that it has the same flexibility as the skin.[14] This method can solve the problem selecting the suitable solvents; also, by applying this method, two drugs can be loaded and released without any interference, depending on the type of the wound and skin injury. The controlled release of drugs can prevent their destructive effects.[15]

In this research study, the core–shell electrospinning method was used to produce the wound dressing of polyglycerol sebacate/polycaprolactone (PGS/PCL) with the potential of releasing curcumin/ciprofloxacin (CUR/CIP) and simvastatin/ciprofloxacin (SIM/CIP) at the wound site. PGS is a polyester polymer prepared from glycerol ($C_3H_8O_3$) and sebacic acid ($C_{10}H_{18}O_4$) by using polycondensation. This tough and biocompatible elastomer has some linear hydrolytic degradation. So, this polymer is appropriate for drug release.[16] It exhibits behaviors similar to collagen and elastin. Therefore, it is more suitable for engineering soft tissues.[17] Polycaprolactone (PCL) is a polymer displaying biocompatibility, biodegradability, and low toxicity. Therefore, it is suitable for tissue engineering. PCL is a semicrystalline and hydrophobic polymer.[18] The unique properties of PCL are excellent mechanical properties, flexibility, biocompatibility, low antigenicity, low melting point (about 60°C), and nontoxicity.[19] In the last decade, some research studies have demonstrated that the main factors in the delayed wound healing are chronic inflammation and bacterial infection due to impeding, proteolysis, angiogenesis, and oxidative stress.[20] CIP is one of the antibacterial agents that can be effective on both Gram-negative and Gram-positive bacteria in wounds and improve the wound healing process.[13,21] Statins are drugs that show various effects such as antioxidant, anti-inflammatory, and immunomodulatory properties.[22] Several studies have also suggested that they can help with wound healing in various animal models.[23,24] Topical use of statins to a wound can help with angiogenesis, lymphangiogenesis, oxidative stress reduction, and immunological modulation. SIM is one of the most frequently used statins, and it has just been discovered to aid wound healing.[25] Nevertheless, due to its limited water solubility and substantial first-pass hepatic metabolism, SIM has very poor oral bioavailability (about 5%). SIM may cause a variety of adverse effects on liver issues when taken orally. As a result, the local delivery of SIM in the wound region decreases the side effects.[23] On the other hand, CUR is a natural polyphenol molecule that has anti-inflammatory and antioxidant properties.[26] CUR can decrease the expression of pro-inflammatory cytokines including IL-6, TNF-α, and so on.[27,28] CUR has recently been proven to be useful in the treatment of wound healing, endothelial damage, and mucosal damage in a number of investigations.[29]

In this study, the fabrication of PGS/PCL composite membranes was investigated by using the core–shell electrospinning method in two different groups based on the drugs loaded into the system consisting of SIM/CIP and CUR/CIP, respectively. The first group was PGS with SIM in the core, and PCL with an appropriate solvent and CIP in the shell part. The second group was PGS with CUR in the core and PCL with CIP in the shell. In both groups, the aim was to evaluate the wound healing effects of natural and synthetic anti-inflammatory drugs (SIM and CUR), and the antibacterial properties were standardized by using CIP.

2 | MATERIALS AND METHODS

The materials used in this study were phosphate-buffered saline (D-PBS, Sigma-Aldrich), chloroform (Merck), dimethyl formamide (DMF, Merck), acetone (Merck), PCL (Sigma-Aldrich), glycerol (99%, Merck), sebacic acid (99%, Merck), CIP powders (Alborz Pharmaceutical Company), SIM powders (Alborz Pharmaceutical Company), and CUR (Sigma-Aldrich).

2.1 | Polymer preparation

According to previous studies, the PGS prepolymer was synthesized by applying the condensation polymerization method.[13,30,31] Therefore, the sebacic acid (99%) and glycerol (99%) were mixed with the molar ratio of 1:1. Then, the mixture was heated at 120°C in the N_2 atmosphere for 24 h. Then, the reactant was kept under vacuum (at 40°C for 24 h).[32] Finally, a viscous and white PGS prepolymer was obtained.

2.2 | Wound dressing preparation via core–shell electrospinning

For preparation of wound dressing membrane without drugs, PCL (12% wt/vol) was dissolved in the chloroform ($CHCl_3$) and acetone (C_3H_6O) (8:2 vol/vol) to prepare the solution of the shell part at 40°C. After that, PGS (30% wt/vol) was dissolved in chloroform ($CHCl_3$) and DMF (C_3H_7NO) (8:2 vol/vol) solvents were added to prepare the core part at around 30°C. This scaffold was prepared via core-shell electrospinning with the initial selection parameters (tip-to-collector distance (18 cm), voltage (30 to 35 kV), feed flow rates (PGS (0.2 ml/h) and PCL (1 ml/h), temperature (25°C) and humidity (around 30%)). After selection of the best electrospinning parameters, separate the wound dressing membrane with drugs into two groups. The solution of PGS/PCL with SIM/CIP shows that PCL (12% wt/vol) and CIP (10% vol/vol of PCL) dissolve in the chloroform ($CHCl_3$) and acetone (C_3H_6O) (8:2 vol/vol) solvent to prepare the solution of the shell part at 40°C. Similarly, the PGS (30% wt/vol) and SIM powders (5% vol/vol of PGS) were dissolved in chloroform ($CHCl_3$) and DMF (C_3H_7NO) (8:2 vol/vol) to prepare the core part at around 30°C; then, PGS/PCL with SIM/CIP membrane was prepared via core–shell electrospinning with parameter information such as collector distance (18 cm), voltage (35 kV), and feed flow rates (core [0.2 ml/h]/shell [1 ml/h], temperature [25°C], and humidity [around 30%]). The second group of wound dressing was prepared in the same way by applying PCL (12% wt/vol) and the CIP powder (10% vol/vol of PCL) dissolved in the chloroform ($CHCl_3$) and acetone (C_3H_6O) (8:2 vol/vol) to prepare the shell solution at 40°C. PGS (30% wt/vol) and the CUR powder (5% vol/vol of PGS) were dissolved in chloroform ($CHCl_3$) and DMF (C_3H_7NO) (8:2 vol/vol) to prepare the solution of the core part at around 30°C. Figure 1 shows the schematic of the preparation of the wound dressing containing SIM/CIP and CUR/CIP for the in vivo test.

2.3 | Characterization of the drug-loaded PGS/PCL wound dressing

2.3.1 | Chemical characterization

Fourier transform infrared (FTIR) spectroscopy (JASCO 6300) in the range of 400–4000 cm^{-1} was applied to stabilize the chemical characteristics of the drug-containing and drug-free wound dressings, as well as the PGS prepolymer.

2.3.2 | Morphology

TEM (Zeiss-EM10C, Germany) was applied to study the core/shell structure of the coaxially electrospun fibers. The samples were prepared based on the TEM sample preparation protocol.[33]

2.3.3 | Swelling ability

To measure the swelling ability of the samples, they were prepared in a suitable size (20 × 5 mm^2). Before the fibers were immersed in PBS

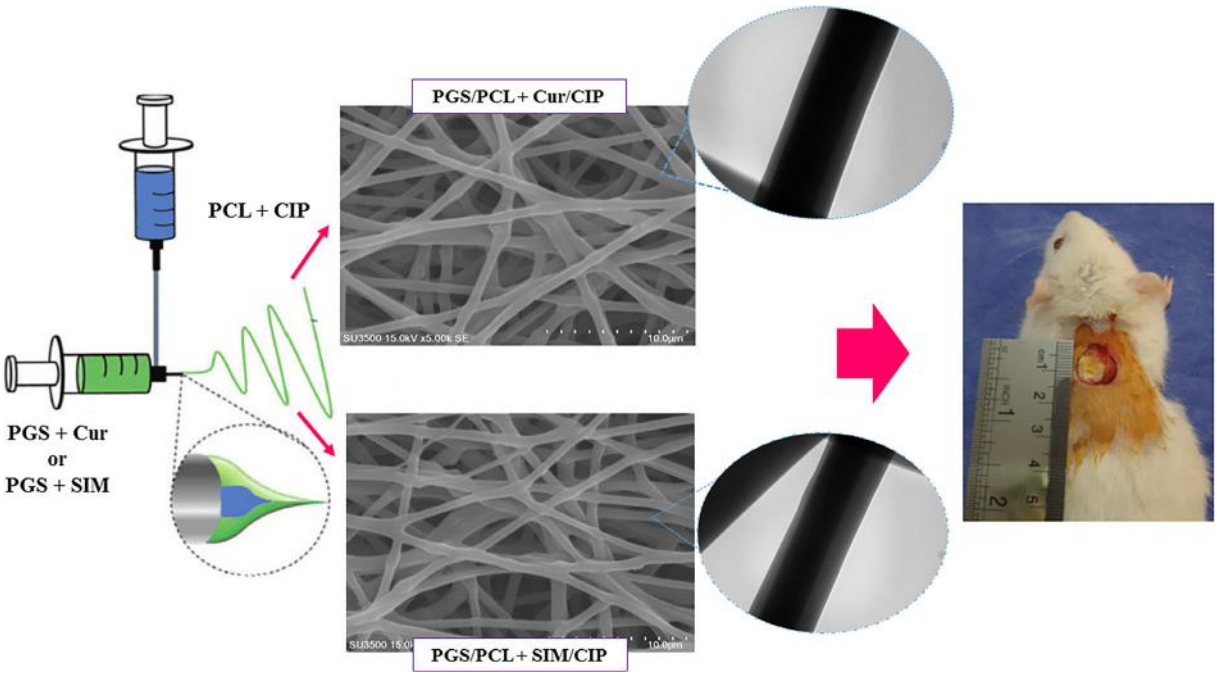

FIGURE 1 Schematic of the preparation and morphology structure of the PGS/PCL with SIM/CIP and PGS/PCL with CUR/CIP for in vivo wound healing process. CIP, ciprofloxacin; CUR, curcumin; PCL, polycaprolactone; PGS, polyglycerol sebacate; SIM, simvastatin

for 60 h, the wet weight (m_w) of the fibers was recorded; then, their dry weights (m_d) were calculated.[34-37] After that, the swelling ability was measured by using the following equation:

$$\text{Swelling}\% = \frac{m_w - m_d}{m_d} \times 100. \quad (1)$$

In this equation, m_w is the wet sample mass and m_d is the dry sample mass. The test was repeated for the two groups of wound dressings three times ($n = 3$).

2.3.4 | Drug release assay

To analyze the drug release assay from the fibers containing SIM/CIP and CUR/CIP, the samples (2.5×2.5 cm^2) were put in 10 ml of PBS ($n = 3$). Then, the samples were moved into a shaker incubator to evaluate the drug entrapment efficiency (at around 37°C, 24 h). Also, the samples (in PBS) were moved into an incubator (at around 37°C, 150 h). Then, after immersion in PBS different times including 15 min, 30 min, 1, 2, 4, 6, 12, 24, 48, 72, and 96 h, a known volume of the solution of the samples in PBS was used to determine the release kinetics of CIP, CUR, and SIM by using UV–VIS spectrophotometry (Shimadzu, Japan). The absorbance peaks of the drugs at 249, 271, and 360 nm wavelengths for SIM, CIP, and CUR were recorded.

2.3.5 | Cell viability

Human skin fibroblast (HSF 1184, Pasteur Institute of Tehran, Iran) cells were cultured in Dulbecco's modified Eagle's medium (DMEM, Sigma) supplemented with 10% fetal bovine serum (Gibco), penicillin/streptomycin mixture (1%, Sigma) in a 5% CO_2 environment at 37°C for 5 days, and the culture medium was changed every days. Electrospun PGS/PCL core–shell nanofibers, PGS/PCL with SIM/CIP, and PGS/PCL with CUR/CIP were sterilized for 2 h with UV radiation, washed three times with PBS, and then submerged in culture media overnight before cell seeding. Confluent cells were trypsinized, and dissociated cells were centrifuged and seeded at a density of 6×10^4 cells on electrospun scaffolds and tissue culture polystyrene as a control. The cell viability was evaluated through the reduction of (3-[4,5 dimethylthiazol-2-yl]-2,5 diphenyl tetrazolium bromide) (MTT) into a formazan dye by live cells. According to the protocol of the MTT assay, cell-seeded scaffolds were washed with PBS after 1, 3, and 5 days and treated with MTT solution (5 mg/ml of MTT reagent [Sigma-Aldrich] in PBS) for 4 h. The solution was then removed, and 100 μl of DMSO was added to each well for 2 h to dissolve the formazan crystals. A microplate reader (BioTek, FLX800) was used to measure the optical density of each well at 560 nm ($n = 3$). In general, it can be said that with increasing the number of cells and their metabolism, the amount of formazan changes in such a way that the optical density increases, which in fact indicates an increase in cell viability.

The morphology and attachment of the HSF cells on the wound dressing were investigated by scanning electron microscopy (SEM) after the 5 days cell culture. Cell cultured samples were washed in PBS, fixed for 3 h with 3% glutaraldehyde (4%, Sigma), rinsed with distilled water, and dehydrated using a graded series of ethanol solutions (50%–100% [vol/vol]). SEM was used to examine completely dried specimens that had been sputter coated with platinum.

2.3.6 | Wound healing assay

The in vivo wound healing was evaluated by using the 15 adult female rats with an average weight of 240–280 g and 4 months old. The rats were taken from the Basic Medical Science Research Center Histogenotech. Animals were kept at a suitable temperature (27°C) and humidity (40%). At first, the rats were anesthetized by the injection of 50 mg/kg body weight ketamine (10%) and 5 mg per kg body weight zeylerin (2%). After that, the hair of the back area of the animals was shaved. The skin area was disinfected with alcohol, and a wound (1×1 cm^2 and full thickness) was produced on the back (lumbar dorsum) of each rat. The animals were randomly divided into three groups with five rats in each group. In the control group, the wounds were not treated (group A). The second group was treated with a wound dressing containing SIM/CIP (group B) and the third group was treated with a wound dressing containing CUR/CIP (group C). Animals were caged individually and provided free access to food and water. All animal experiments were performed according to the guideline approved by the Animal Use and Care Administrative of the Isfahan University of Medical Science.

2.4 | Histometric evaluation

To evaluate the histometry, after the ulcers were created on the days 0, 4, 7, and 14, the rats were anesthetized. After that, the digital camera was used to take the related images. The wound size and rate of wound healing were evaluated. The ImageJ 2017 software was used to measure the size of the wound. Then, the percentage of the wound size was calculated by using Equation (2):

$$\text{Wound size} = \frac{A_0}{A_t} \times 100, \quad (2)$$

where A_0 is the wound size at the initial time and A_t is the wound size at time t.

2.5 | Histopathology evaluation

To analyze the wound histology, on Day 14 of the experiment, the wounds healed on the back of the animals in each group were cut with some healthy tissue surrounding the wound. The samples were fixed in 10% formalin and then fixed in paraffin. Then, the microtome-

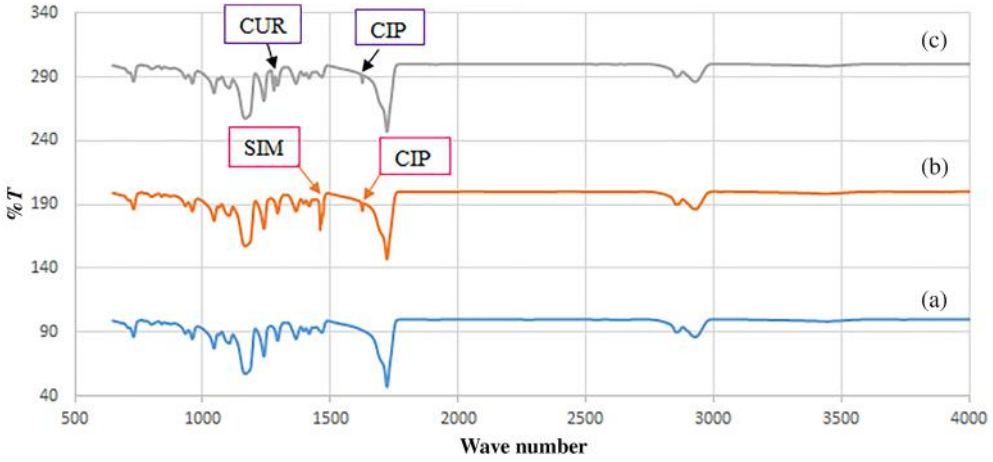

FIGURE 2 Fourier transform infrared (FTIR) spectra in the range of 400–4000 cm^{-1} of (A) PGS/PCL, (B) PGS/PCL with SIM/CIP, and (C) PGS/PCL with CUR/CIP samples. CIP, ciprofloxacin; CUR, curcumin; PCL, polycaprolactone; PGS, polyglycerol sebacate; SIM, simvastatin

cutting machine was used to prepare the molded tissues with the following sections and a suitable thickness (5 μm). The cuts were done transversely; they contained the restored skin. Then hematoxylin and eosin (H&E) was used to stain the cuts of the samples. After that, they were dehydrated and mounted. After that, a digital light microscope (Olympus, Japan) was used to take the histological photographs.

2.6 | Evaluation of collagen levels

Collagen levels were measured in each group by using the real-time PCR. Primer design was first performed; then the total RNA was extracted from the tissues and transformed into cDNA by using the reverse transcriptase (RT) enzyme. The resulting cDNA was treated with the DNase I enzyme to remove the genomic DNA; then cDNA was replicated by applying the PCR real-time method. Therefore, cDNA was amplified by the PCR method and then analyzed based on glyceraldehyde-3-phosphate dehydrogenase (GAPDH) expression.

2.7 | Statistical analysis

Test results were presented as means ± SD. The one-way analysis of variance was used, and differences were considered statistically significant at $p < .05$.

3 | RESULTS

3.1 | Chemical characterization of PGS/PCL wound dressings

Figure 2 shows the FTIR spectra of all samples. The spectrum (a) is related to the PGS/PCL wound dressing. The peak around 3458 cm^{-1} was related to the hydroxyl group and those around 2925 and 2853 cm^{-1} could be attributed to methyl and alkane groups of PGS. Also, the peak at around 1171 cm^{-1} from C—O and the peak around 1731 cm^{-1} from the C═O functional group were related to PGS (Figure 2(A)).[13,38] Some peaks including 1060 cm^{-1} (C—O), 1238 cm^{-1} (C—O—C), and 1722 cm^{-1} (C═O) belonged to PCL.[39]

Figure 2(B) shows the spectra of the wound dressing containing SIM/CIP. The peak around 1464.67 cm^{-1} from the C—H bending vibration of methyl and methylene was related to SIM; the peak around 1624 cm^{-1} belonged to CIP.[40,41] Figure 2(C) shows the peaks related to the wound dressing containing CUR/CIP. The peak around 1277 cm^{-1} revealed the bending vibration of the C—O phenolic band of CUR; the peak around 1624 cm^{-1} belonged to CIP.[40,42]

3.2 | Morphology

Figure 3 shows the TEM images of the PGS/PCL wound dressing containing CUR/CIP (a) and the SIM/CIP (b) core/shell structure. A

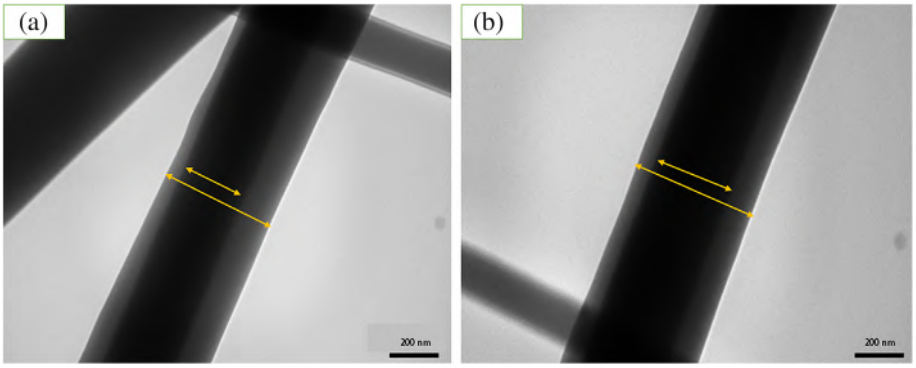

FIGURE 3 Transmission electron microscopy (TEM) images for identifying the morphology and core–shell structure in wound dressing containing (A) SIM/CIP and (B) CUR/CIP. CIP, ciprofloxacin; CUR, curcumin; SIM, simvastatin

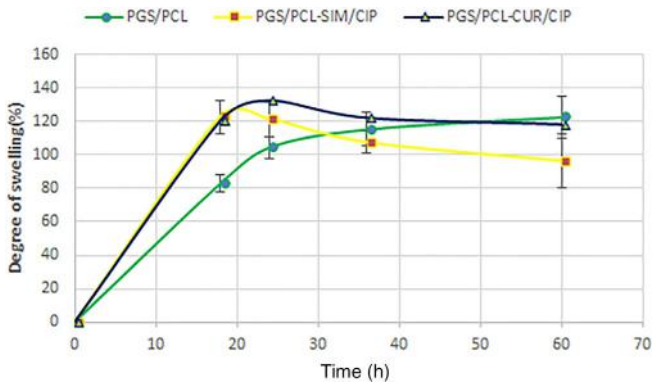

FIGURE 4 Degree of swelling ratios (%) of the membranes (PGS/PCL, PGS/PCL with SIM/CIP, and PGS/PCL with CUR/CIP) related by time ($n = 3$). CIP, ciprofloxacin; CUR, curcumin; PCL, polycaprolactone; PGS, polyglycerol sebacate; SIM, simvastatin

previous study had shown the major role of the flow rate in the electrospinning process of the polymer solutions.[13] The suitable flow rate for electrospinning the drug-containing PGS/PCL fibers is 0.2:1 ml/h. According to Figure 3, a separate core and shell structure was created in the structure of both electrospun wound dressings. It could be clearly observed that the core was completely encapsulated in the shell. Therefore, the electrospun fibers were able to load two different drugs (CUR/CIP and SIM/CIP) at the same time. On the other hand, the average diameter of PGS/PCL containing SIM/CIP (Figure 3(A)) was about 530 ± 40.6 nm; in PGS/PCL containing CUR/-CIP (Figure 3(B)), this was about 575 ± 81.4 nm. It was, therefore, despite the changes in the drugs in the core of the fibers, the fiber diameters did not differ significantly ($p > 0.05$).

3.3 | Water uptake (swelling) ability of wound dressing

The capacity of water absorption is one of the factors that determine the appropriate polymeric materials for the fabrication of wound dressing.[43] This parameter showed the amounts of absorbed exudates in the wound site.[44] The degree of swelling in wound dressing was analyzed after removal from PBS to determine the increasing weight. Figure 4 shows the water absorption results in the PGS/PCL groups. After measuring the water uptake of the samples, the results demonstrated that in the first 20 h, the weight of the membrane in three groups was significantly increased. In addition, in the first 24 h, the rate of water absorption by the wound dressing containing the drugs was higher than that of the control group (PGS/PCL). The percentage of the swelling ability of the wound dressing containing SIM/CIP was 121% and 132%, respectively, in 24 h. It seems that the presence of CUR compared to SIM has caused more water absorption, so that after 60 h, the fastest swelling rate is related to the membrane containing CUR/CIP and then the SIM/CIP group.

3.4 | Drug release studies of the wound dressing

The absorption spectra of CIP, SIM, and CUR in the PBS medium were in the range of 200–600 nm, and the maximum absorption was 270, 249, and 360 nm, respectively. Depending on the absorption rate of each drugs at the specified concentration, the drugs loading of the wound dressing made CIP, SIM, and CUR equal to 30.25, 25.58, and 29.52 μg/ml, respectively. The drug release of the wound dressing in the PBS medium has been shown in Figure 5. The drug release rate of CIP was 65% in the first 24 h; therefore, based on the drug release rate, it could be appropriate for treating the wound and preventing the infection at the wound site. On the other hand, the drug release rate of SIM was slow at the first 24 h; then, after 3 days, the highest drug release was observed.

Therefore, the wound dressing containing SIM/CIP showed the controlled drug release; so, at first, CIP was released, preventing the infection at the wound site; then the SIM was released, reducing the wound inflammation.

In the wound dressing containing CUR/CIP, the drug release rate of CIP was 60% in the first 24 h, while that of CUR was 70% after 24 h. Compared to SIM in the first group of the known wound

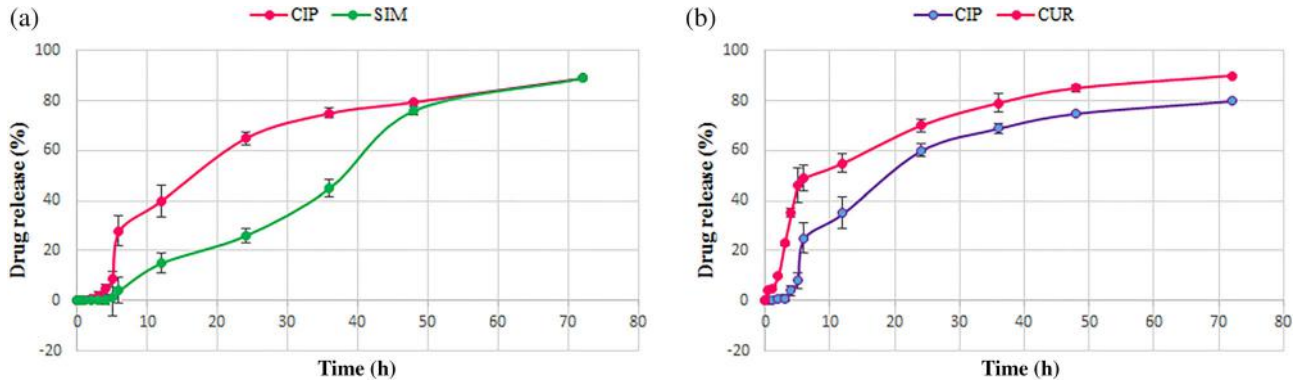

FIGURE 5 In vitro drug release profiles of wound dressing containing (A) SIM/CIP and (B) CUR/CIP in PBS (pH = 7.4) at 37°C ($n = 9$). CIP, ciprofloxacin; CUR, curcumin; PBS, phosphate-buffered saline; SIM, simvastatin

dressing, the drug release rate of CUR was faster given the hydrophilicity of CUR.

3.5 | Cell viability

The results of the MTT assay demonstrated the cell viability and proliferation of the known wound dressing. Figure 6(A) shows the MTT results of the control and wound dressing with or without drugs. According to this figure, the wound dressing in three groups including PGS/PCL, PGS/PCL, which contained SIM/CIP, and PGS/PCL with CUR/CIP did not show any cytotoxicity on the HSF cells because the amount of the HSF cells was increased after 3 and 5 days of the cell culture (Figure 6(A)).

Finally, Figure 6(B,C) shows the SEM images of the PGS/PCL wound dressing containing CUR/CIP (B) and SIM/CIP (C). The HSF cells were attached on both wound dressings after 5 days of the cell culture because these two had high hydrophilicity for the cell adhesion.

3.6 | Wound healing

The process of the wound healing by the given wound dressing was observed for 14 days. Their related images were taken upon 0, 4, 8, and 14 days after operation of the wound (Figure 7 shows that during the first 4 days, in the CUR/CIP group, the wound healing area was markedly larger than in control and no significant difference was observed between SIM/CIP and CUR/CIP groups.

The process of the wound closure by the wound dressing containing CIP and SIM was almost completed in 14 days, while the mean wound closure area was about 65% of the wound in the same time. There was a significant difference between SIM/CIP (96% ± 4%) and the control groups (73% ± 6%).

3.7 | Histopathological evaluation

Histological analysis of the wounds was performed on Day 14 after the operation of the wound. The results have been shown in Figure 8. In the CUR/CIP group, the epidermis was a thin layer in the wound area. Collagen was observed normally in some areas of the dermis; however, there were no collagen layers in all areas; so, it was not possible to separate the dermis layer from the hypodermis in the most damaged areas. The thickness of the epidermal layer was non-uniform, and no hair, sweat glands, and fat could be found in the wound area.

In the SIM/CIP group, skin layers including epidermis, dermis, and hypodermis were observed separately. In this group, the thickness of the epidermis layer was observed uniformly. In the dermis region, the collagen layers were observed in a parallel arrangement with the pressure level in the skin area, which was similar to the healthy skin. In the hypodermis section, fat vacuoles, blood vessels, and subcutaneous muscle were observed (Figures 8).

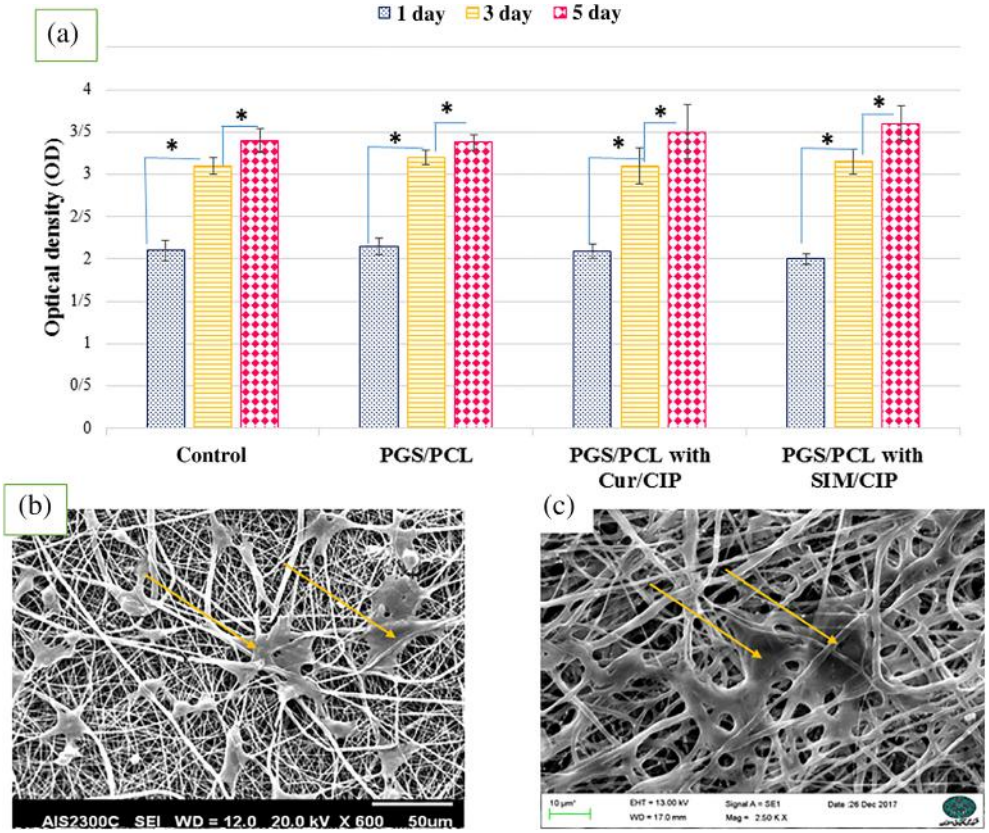

FIGURE 6 HSF cells' viability expressed by the optical density of the cells using the MTT assay for control, PGS/PCL, PGS/PCL with SIM/CIP, and PGS/PCL with CUR/CIP groups after 1, 3, and 5 days cell culture ($n = 3$, $^*p < .05$) (A). The proliferation and SEM images of HSF after 5 days culturing on wound dressing containing CUR/CIP (B), and SIM/CIP (C). CIP, ciprofloxacin; CUR, curcumin; HSF, human skin fibroblast; MTT, 3-[4,5 dimethylthiazol-2-yl]-2,5 diphenyl tetrazolium bromide; PCL, polycaprolactone; PGS, polyglycerol sebacate; SEM, scanning electron microscopy; SIM, simvastatin

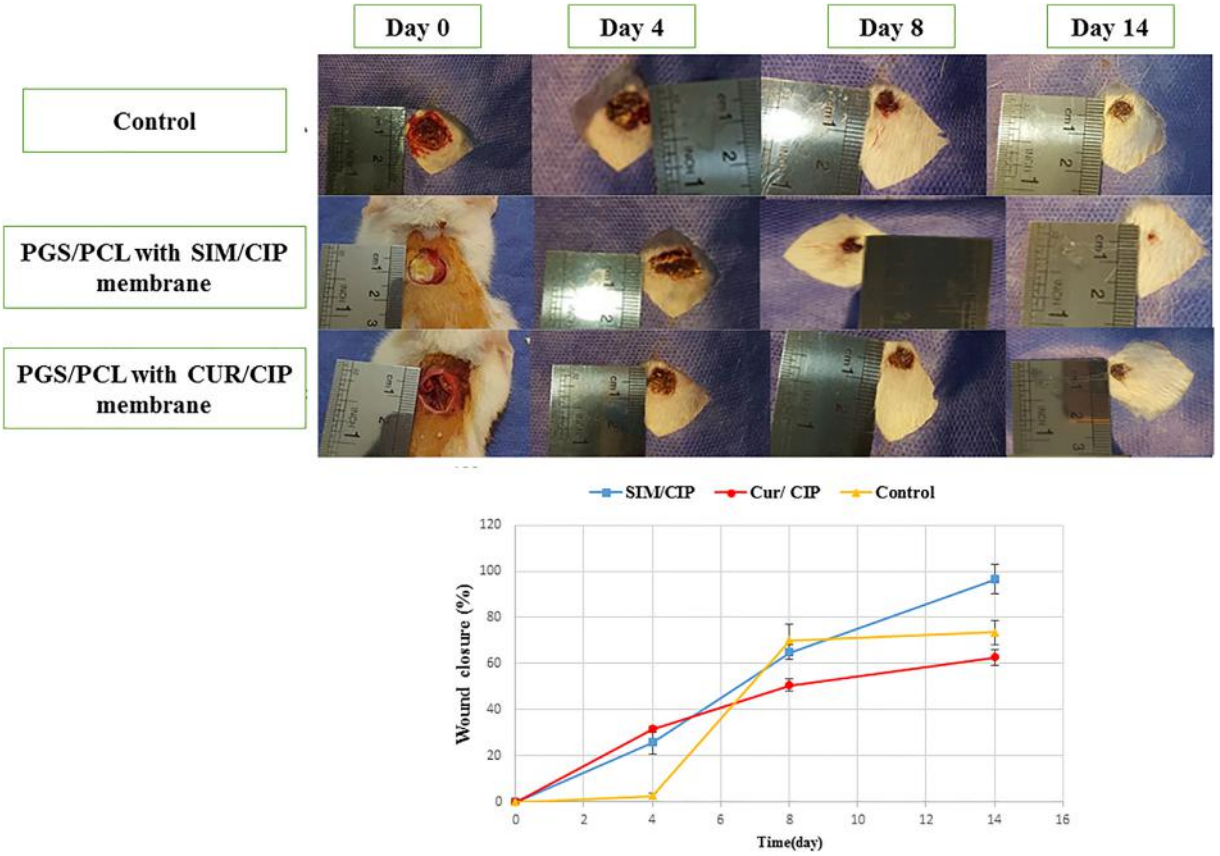

FIGURE 7 The wound healing effect in vivo ($n = 5$): (A) macroscopic appearances of the treated wounds at the 0, 4, 8, and 14 days after creation of the wound, (B) histograms comparing the wound size percentages of the wound dressings at the end of 4, 8, and 14 days after creation of the wound in three groups (control, wound dressing containing SIM/CIP, and wound dressing containing CUR/CIP). CIP, ciprofloxacin; CUR, curcumin; SIM, simvastatin

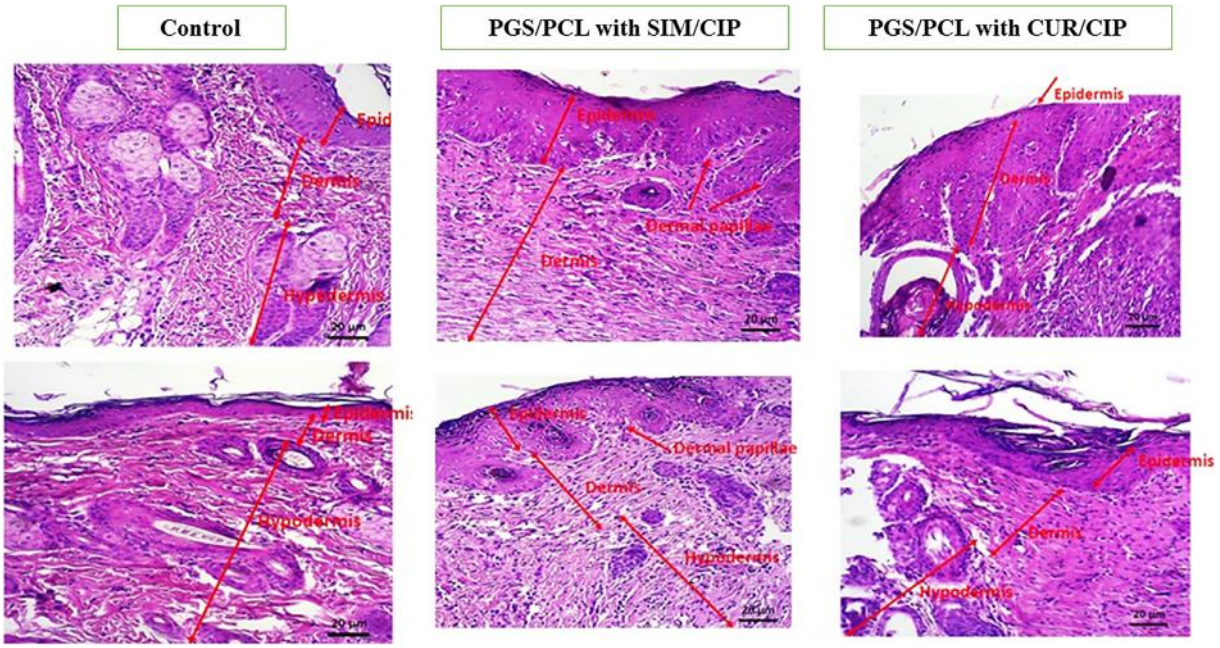

FIGURE 8 The histology analysis of the wound area (epidermis, dermis, hypodermis, fat vacuoles, blood vessels, and subcutaneous muscle) at different groups SIM/CIP, CUR/CIP, and control group after 14 days. CIP, ciprofloxacin; CUR, curcumin; SIM, simvastatin

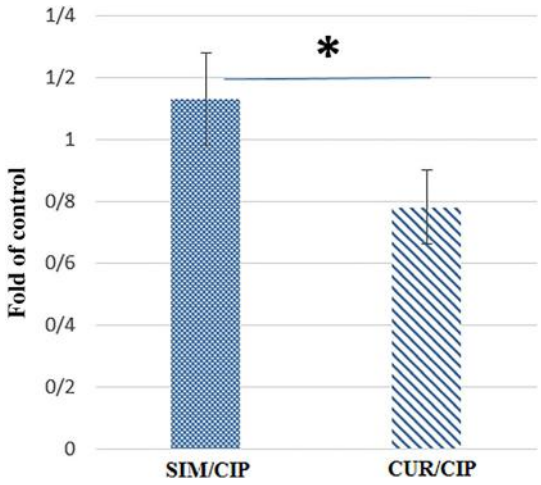

FIGURE 9 Effects of the wound dressing containing SIM/CIP and wound dressing containing CUR/CIP on collagen mRNA expression after 14 days (*$p < 0.05$). CIP, ciprofloxacin; CUR, curcumin; SIM, simvastatin

3.8 | Evaluation of the collagen content

Figure 9 represents the normalized collagen expression level in the wound during the wound healing process in SIM/CIP and CUR/CIP groups after 14 days. The results well demonstrated that there was significant difference between the two groups (wound repaired by the dressing containing SIM/CIP and the one repaired by the one containing CUR/CIP) in the level of collagen ($p < .05$), while no significant difference was found between the control and SIM/CIP groups.

4 | DISCUSSION

In this research, biodegradable dressings made of PGS/PCL containing CUR/CIP and SIM/CIP (as anti-inflammation/anti-infection factors) were prepared by applying the coaxial electrospinning method.

These drugs were selected to control inflammatory mediators and in order to improve the wound healing process. Results of in vitro and in vivo consideration showed that in the CUR-treated wounds, faster wound closure occurred; however, after 14 days, in the wound treated with SIM, the amount of collagen deposition and angiogenesis was higher, such that wound was closed almost completely and the skin layers in this group were formed normally and uniformly.

The FTIR results showed that all drugs of the two wound dressings were located in the core and shell portion, separately, without any changes in the chemical structure of PGS/PCL. Using the core–shell technique can well provide the ability to load two drugs without interfering in one system.[13,45]

The results of fiber morphology evaluation (TEM) showed the formation of two core and shell regions separately. Also, it was clear that despite the changes in the drugs in the core of the fibers, the fiber diameters did not differ significantly ($p > .05$).

An ideal wound dressing requires absorption and high swelling in order to absorb skin secretions and exudates.[46,47] In this study, the percentage of the swelling ability of the wound dressing containing SIM/CIP and CUR/CIP was 121% and 132%, respectively, in 24 h. In general, the inner core of the sample is made up of a hydrophilic polymer (PGS), while the outside shell is made up of a hydrophobic polymer (PCL). The electrospun PGS/PCL wound dressing has a porous structure with a large specific surface area, allowing liquids to permeate and produce swelling. So that, the reason of increasing water absorption by the drug-containing wound dressing was the placement of the molecules of water in the structure when the drug was released. Comparing the two groups containing the drugs and the drug-free sample, it can be said that the presence of a hydrophilic drug such as CIP in the fiber shell has increased water penetration compared to the drug-free sample. On the other hand, the presence of hydrophobic drugs such as SIM in the fiber core between the two groups containing drugs has slowed the decreasing degree of the swelling process compared to CUR. According to the previous studies, when the percentage of the swelling ability of the wound dressing is in the range of 100%–900% during 24 h, the wound dressing is ideal.[48] Therefore, based on the previous study, the wound dressing containing SIM/CIP and CUR/CIP could be regarded as the ideal for the wounds with none to low exudates.[49]

Other important factors for wound dressing are antibacterial properties. Bacterial wound infection is destructive to wound healing, and severe bacterial infections can lead to systemic problems. As a result, avoiding wound infection by wound dressings with antibacterial activity is critical to complete wound regeneration. CIP is a powerful antibacterial drug that may be used to treat a variety of skin defects and accelerate wound healing process.[50-52] On the other hand, angiogenesis and inflammation are other problems in wound healing process that needed external drugs or factors to promoting wound healing. SIM is an anti-inflammatory and antioxidant drug that has a critical function in the control of angiogenesis, treatment of acute inflammation, improving diabetic wound healing, and increasing the formation of new blood vessels when it is released locally.[53] After that, one of the natural materials more effective on wound healing is CUR, which has anti-inflammatory and antioxidant effects.[54] One of the most important results of this study is the process of releasing drugs from the fibers. The release rate of CIP was 65% in the first 24 h and the release rate of SIM was slow at the first 24 h. Therefore, the wound dressing containing SIM/CIP showed the controlled drug release; so, at first, CIP was released, preventing the infection at the wound site; then the SIM was released, reducing the wound inflammation. The location of the SIM in the core portion could be taken as the first reason for the controlled drug release of the fibers (wound dressing); another reason is the hydrophobicity of the SIM. Moreover, polymer degradation rate is an important parameter that affects the drug release rate. In hydrolytic degradation process of the PGS, water molecules attract to the amorphous region and cause hydrolytic scission of the ester groups.[55] The release of shortened chains from the structure causes more water penetration and leads to the release of even hydrophobic drug molecules from the fibers. Replacement of

PGS polymer containing the hydrophobic drug SIM in the core and covering it with the hydrophobic shell of PCL can be one of the reasons for the delay in the release of SIM.

In the wound dressing containing CUR/CIP, the drug release rate of CIP was 60% in the first 24 h, while that of CUR was 70% after 24 h. Compared to SIM in the first group of the known wound dressing, the drug release rate of CUR was faster given the hydrophilicity of CUR. The previous studies have also shown that the anti-inflammatory drug can control the process of recovery and treatment of the wound, when it is released slowly within 2 days. The fast release of the anti-inflammatory drugs could show an adverse effect and delay the wound healing process.[56,57] Accordingly, the wound dressing containing SIM/CIP could well control the infection at the wound site in the first 24 h; after that, it can improve the healing process by releasing 60% of SIM in 48 h. On the other hand, in the wound dressing containing CUR/CIP, CUR was released in the highest level after 36 h. The faster release of the CUR, as compared with the SIM, could be due to the more solubility of CUR in water (as compared to the lipophilic SIM).

According to previous research studies, if the concentration of CUR, SIM, and CIP is more than 35, 40, and 60 μg/ml, respectively, it leads to cytotoxicity.[13,52,58,59] In the present study, the amount of each drug in the structure was less than these values. For this reason, no toxicity was shown in all samples and wound dressing in the three groups; so, they could improve cell growth and proliferation. Also, there was no significant difference between the cell's viability of the two wound dressings with different drugs. As a result, these wound dressings could improve the attachment and proliferation of the HSF cells. This agrees with other studies that showed the pore size and surface area of the PCL-based membranes lead to initial cell attachment and restrict by the hydrophobicity of the PCL fibers.[60,61]

In vivo study showed that the better response of the wound closer in the wound dressing containing SIM/CIP and CUR/CIP, as compared with the control, was due to the anti-inflammatory effect of CUR and SIM. SIM has been shown to increase angiogenesis via the vascular endothelial growth factor (VEGF) and reduction of chronic inflammation in the wound area.[62] Yen et al. also reported that CUR treatment increased the expression of TNF-α and protein levels, consequently accelerating wound healing in the early phase of treatment.[63] Moreover, SIM is known as one of the best anti-inflammatory drugs.[62] These results clearly showed the effects of CIP and SIM on the improvement of the wound healing efficiency of the wound dressing containing CIP and SIM after 14 days of treatment. On the other hand, in the hypodermis section, fat vacuoles, blood vessels, and subcutaneous muscle were observed in the SIM/CIP group. The effective healing was, therefore, demonstrated by the appearance of the hair follicles.[64] According to Mun et al., SIM could suppress the TGF-β1-induced production of Type I collagen and prevent the excessive scar formation.[65]

The major structural protein present in the dermal layer of the skin is collagen.[66] Liu et al. also revealed that the collagen deposition was enhanced in the granulation tissue of the wounds treated with SIM.[67] The results obtained in the present research were in agreement with those of Asai et al.[68] They reported that histologic wounds treated with SIM showed significantly higher degrees of the maturation of the granulation tissue, collagen deposition, and re-epithelialization, in addition to neovascularization.[68]

Many efforts have been made to improve the wound healing process by modifying the various stages of wound healing. These include protecting wound tissue from bacterial infection, reducing long-term inflammation, and differentiating fibroblasts for wound regeneration and wound closure.[63]

Various research studies have revealed that SIM and CUR could accelerate wound healing via different pathways. CUR is usually released in the wound site with a burst pattern, affecting the inflammatory process and increasing the differentiation of fibroblasts to myofibroblasts. These cells play a major role in the contraction and proliferation phases of wound healing.[63] SIM is an anti-inflammatory agent showing a beneficial role in wound healing via its angiogenic, antifibrotic, and immunomodulatory effects, as well as accelerating the wound healing process.[69]

A comparison of the results obtained by wound treatment using the dressing containing CUR and SIM was done in this study as well. Since the control of bacterial infection in the wound area is one of the important factors affecting wound healing, CIP was added to both dressings to standardize the control of this parameter. Our previous research studies had demonstrated that the release of CIP from the electrospun wound dressing could successfully prevent the gram-positive and gram-negative bacterial activities.[13,43,70]

The results of the present study showed that in the CUR-treated wounds, a faster wound closure occurred; however, after 14 days, in the wound treated with SIM, the amount of collagen deposition and angiogenesis was higher, such that wound was closed almost completely and the skin layers in this group were formed normally and uniformly. It seems, therefore, that the use of SIM and CUR in a wound dressing could simultaneously play a synergistic role in the wound repair and remodeling, thus improving the new tissue formation and healing time, and preventing scar formation. This could be considered as a topic in the future for the in vitro and in vivo studies.

5 | CONCLUSION

To summarize, novel electrospun PGS/PCL wound dressings with SIM/CIP and CUR/CIP were prepared successfully by using the core–shell electrospinning method. Both of these wound dressing were suitable for low exuding wounds. CUR showed burst release and caused a faster wound contraction while SIM showed a slow release pattern with at least 24 h delay. In the in vivo study, wound healing was almost completed during 14 days, only in SIM/CIP groups. Comparing the wound healing process in these two dressings, it could be concluded that the simultaneous use of CUR and SIM may lead to faster and more effective wound healing, which should be more considered in future studies.

ACKNOWLEDGMENTS

This research study has been supported by funding from NIMAD (National Institute for Medical Research Development Islamic Republic of Iran) grant (grant number: 963505).

DATA AVAILABILITY STATEMENT

The data that support the findings of this study are available from the corresponding author upon reasonable request.

REFERENCES

1. Groeber F, Holeiter M, Hampel M, Hinderer S, Schenke-Layland K. Skin tissue engineering—in vivo and in vitro applications. *Adv Drug Deliv Rev*. 2011;*63*(4):352-366.
2. Li M, Liang Y, He J, Zhang H, Guo B. Two-pronged strategy of biomechanically active and biochemically multifunctional hydrogel wound dressing to accelerate wound closure and wound healing. *Chem Mater*. 2020;*32*(23):9937-9953.
3. Morgado PI, Aguiar-Ricardo A, Correia IJ. Asymmetric membranes as ideal wound dressings: an overview on production methods, structure, properties and performance relationship. *J Membr Sci*. 2015;*490*:139-151.
4. Shevchenko RV, James SL, James SE. A review of tissue-engineered skin bioconstructs available for skin reconstruction. *J R Soc Interf*. 2009;*43*:229-258.
5. Huang Y, Zhao X, Zhang Z, et al. Degradable gelatin-based IPN cryogel hemostat for rapidly stopping deep noncompressible hemorrhage and simultaneously improving wound healing. *Chem Mater*. 2020;*32*(15):6595-6610.
6. Chen T-Y, Wen T-K, Dai N-T, Hsu S. Cryogel/hydrogel biomaterials and acupuncture combined to promote diabetic skin wound healing through immunomodulation. *Biomaterials*. 2021;*269*:120608.
7. Zhao X, Liang Y, Guo B, Yin Z, Zhu D, Han Y. Injectable dry cryogels with excellent blood-sucking expansion and blood clotting to cease hemorrhage for lethal deep-wounds, coagulopathy and tissue regeneration. *Chem Eng J*. 2021;*403*:126329.
8. Boateng JS, Matthews KH, Stevens HNE, Eccleston GM. Wound healing dressings and drug delivery systems: a review. *J Pharm Sci*. 2008;*97*(8):2892-2923.
9. Andreu V, Mendoza G, Arruebo M, Irusta S. Smart dressings based on nanostructured fibers containing natural origin antimicrobial, anti-inflammatory, and regenerative compounds. *Materials*. 2015;*8*(8):5154-5193.
10. He J, Liang Y, Shi M, Guo B. Anti-oxidant electroactive and antibacterial nanofibrous wound dressings based on poly (ε-caprolactone)/quaternized chitosan-graft-polyaniline for full-thickness skin wound healing. *Chem Eng J*. 2020;*385*:464.
11. Hu X, Liu S, Zhou G, Huang Y, Xie Z, Jing X. Electrospinning of polymeric nanofibers for drug delivery applications. *J Control Release*. 2014;*185*:12-21.
12. Rieger KA, Birch NP, Schiffman JD. Designing electrospun nanofiber mats to promote wound healing–a review. *J Mater Chem B*. 2013;*1*(36):4531-4541.
13. Heydari P, Varshosaz J, Zargar Kharazi A, Karbasi S. Preparation and evaluation of poly glycerol sebacate/poly hydroxy butyrate core-shell electrospun nanofibers with sequentially release of ciprofloxacin and simvastatin in wound dressings. *Polym Advan Technol*. 2018;*29*:1795-1803.
14. Xu B, Rollo B, Stamp LA, et al. Non-linear elasticity of core/shell spun PGS/PLLA fibres and their effect on cell proliferation. *Biomaterials*. 2013;*34*(27):6306-6317.
15. Perez RA, Kim H-W. Core–shell designed scaffolds for drug delivery and tissue engineering. *Acta Biomater*. 2015;*21*:2-19.
16. Sant S, Khademhosseini A. Fabrication and characterization of tough elastomeric fibrous scaffolds for tissue engineering applications. Paper presented at: 2010 Annual International Conference of the IEEE Engineering in Medicine and Biology Society, EMBC'10. 2010: 3546-3548. doi:https://doi.org/10.1109/IEMBS.2010.5627486
17. Rai R, Tallawi M, Grigore A, Boccaccini AR. Synthesis, properties and biomedical applications of poly(glycerol sebacate) (PGS): a review. *Prog Polym Sci*. 2012;*37*(8):1051-1078. https://doi.org/10.1016/j.progpolymsci.2012.02.001
18. Guo B, Ma PX. Synthetic biodegradable functional polymers for tissue engineering: a brief review. *Sci China Chem*. 2014;*57*(4):490-500.
19. Cheng M-L, Lin Y-R, Lin Z-Z, Liao C-S, Sun Y-M. Physical and transport properties of polyhydroxybutyrate/clay nanocomposite membranes. *Tc (C)*. 2014;*87*(96):87.
20. Costache MC, Qu H, Ducheyne P, Devore DI. Polymer–xerogel composites for controlled release wound dressings. *Biomaterials*. 2010;*31*(24):6336-6343.
21. Marchesan S, Qu Y, Waddington LJ, et al. Self-assembly of ciprofloxacin and a tripeptide into an antimicrobial nanostructured hydrogel. *Biomaterials*. 2013;*34*(14):3678-3687.
22. Rezvanian M, Ng S-F, Alavi T, Ahmad W. In-vivo evaluation of alginate-pectin hydrogel film loaded with simvastatin for diabetic wound healing in streptozotocin-induced diabetic rats. *Int J Biol Macromol*. 2021;*171*:308-319.
23. Abd El-Alim SH, Salama A, Darwish AB. Provesicular elastic carriers of simvastatin for enhanced wound healing activity: an in-vitro/in-vivo study. *Int J Pharm*. 2020;*585*:119470.
24. Ramhormozi P, Ansari JM, Simorgh S, et al. Simvastatin accelerates the healing process of burn wound in Wistar rats through Akt/mTOR signaling pathway. *Ann Anatomy-Anatomischer Anzeiger*. 2021;*236*:151652.
25. Örgül D, Eroğlu H, Tiryaki M, Pınarlı FA, Hekimoglu S. In-vivo evaluation of tissue scaffolds containing simvastatin loaded nanostructured lipid carriers and mesenchymal stem cells in diabetic wound healing. *J Drug Deliv Sci Technol*. 2021;*61*:102140.
26. Wang Y, Ying T, Li J, et al. Hierarchical micro/nanofibrous scaffolds incorporated with curcumin and zinc ion eutectic metal organic frameworks for enhanced diabetic wound healing via anti-oxidant and anti-inflammatory activities. *Chem Eng J*. 2020;*402*:126273.
27. Andrabi SM, Majumder S, Gupta KC, Kumar A. Dextran based amphiphilic nano-hybrid hydrogel system incorporated with curcumin and cerium oxide nanoparticles for wound healing. *Colloids Surf B Biointerfaces*. 2020;*195*:111263.
28. Mohanty C, Pradhan J. A human epidermal growth factor-curcumin bandage bioconjugate loaded with mesenchymal stem cell for in vivo diabetic wound healing. *Mater Sci Eng C*. 2020;*111*:110751.
29. Rezkita F, Wibawa KGP, Nugraha AP. Curcumin loaded chitosan nanoparticle for accelerating the post extraction wound healing in diabetes mellitus patient: a review. *Res J Pharm Tech*. 2020;*13*(2):1039.
30. Li Y, Cook WD, Moorhoff C, Huang W, Chen Q. Synthesis, characterization and properties of biocompatible poly (glycerol sebacate) prepolymer and gel. *Polym Int*. 2013;*62*(4):534-547.
31. Li X, Hong AT, Naskar N, Chung H. Criteria for quick and consistent synthesis of poly(glycerol sebacate) for tailored mechanical properties. doi:https://doi.org/10.1021/acs.biomac.5b00018, *16*, 1525, 1533
32. Xu B, Li Y, Zhu C, Cook WD, Forsythe J, Chen Q. Fabrication, mechanical properties and cytocompatibility of elastomeric nanofibrous mats of poly(glycerol sebacate). *Eur Polym J*. 2015;*64*:79-92. https://doi.org/10.1016/j.eurpolymj.2014.12.008
33. Ding Y, Dou C, Chang S, et al. Core–shell eudragit s100 nanofibers prepared via triaxial electrospinning to provide a colon-targeted extended drug release. *Polymers*. 2020;*12*(9):2034.
34. Chen C-K, Liao M-G, Wu Y-L, Fang Z-Y, Chen J-A. Preparation of highly swelling/antibacterial cross-linked N-maleoyl-functional

chitosan/polyethylene oxide nanofiber meshes for controlled antibiotic release. *Mol Pharm*. 2020;*17*(9):3461-3476.
35. Vargas EAT, do Vale Baracho NC, De Brito J, De Queiroz AAA. Hyperbranched polyglycerol electrospun nanofibers for wound dressing applications. *Acta Biomater*. 2010;*6*(3):1069-1078.
36. Lee KY, Mooney DJ. Alginate: properties and biomedical applications. *Prog Polym Sci*. 2012;*37*(1):106-126.
37. Sadeghianmaryan A, Sardroud HA, Allafasghari S, et al. Electrospinning of polyurethane/graphene oxide for skin wound dressing and its in vitro characterization. *J Biomater Appl*. 2020;*35*(1):135-145.
38. Kharaziha M, Nikkhah M, Shin S-R, et al. PGS: gelatin nanofibrous scaffolds with tunable mechanical and structural properties for engineering cardiac tissues. *Biomaterials*. 2013;*34*(27):6355-6366.
39. Kharazi AZ, Atari M, Vatankhah E, Javanmard SH. A nanofibrous bilayered scaffold for tissue engineering of small-diameter blood vessels. *Polym Advan Technol*. 2018;*29*(12):3151-3158.
40. Wu Q, Li Z, Hong H, Yin K, Tie L. Adsorption and intercalation of ciprofloxacin on montmorillonite. *Appl Clay Sci*. 2010;*50*(2):204-211.
41. Mandal D, Ojha PK, Nandy BC, Ghosh LK. Effect of carriers on solid dispersions of simvastatin (Sim): physico-chemical characterizations and dissolution studies. *Der Pharm Lett*. 2010;*2*(4):47-56.
42. Krausz AE, Adler BL, Cabral V, et al. Curcumin-encapsulated nanoparticles as innovative antimicrobial and wound healing agent. *Nanomed Nanotechnol Biol Med*. 2015;*11*(1):195-206.
43. Shirazaki P, Varshosaz J, Kharazi AZ. Electrospun gelatin/poly (glycerol sebacate) membrane with controlled release of antibiotics for wound dressing. *Adv Biomed Res*. 2017;*6*:105-124.
44. Zhong SP, Zhang YZ, Lim CT. Tissue scaffolds for skin wound healing and dermal reconstruction. *Wiley Interdiscip Rev Nanomed Nanobiotechnol*. 2010;*2*(5):510-525. https://doi.org/10.1002/wnan.100
45. Nguyen TTT, Chung OH, Park JS. Coaxial electrospun poly(lactic acid)/chitosan (core/shell) composite nanofibers and their antibacterial activity. *Carbohydr Polym*. 2011;*86*(4):1799-1806. https://doi.org/10.1016/j.carbpol.2011.07.014
46. Hoseinpour Najar M, Minaiyan M, Taheri A. Preparation and in vivo evaluation of a novel gel-based wound dressing using arginine–alginate surface-modified chitosan nanofibers. *J Biomater Appl*. 2018;*32*(6):689-701.
47. Wang C, Wang M, Xu T, et al. Engineering bioactive self-healing antibacterial exosomes hydrogel for promoting chronic diabetic wound healing and complete skin regeneration. *Theranostics*. 2019;*9*(1):65-76.
48. Shin YC, Shin D, Lee EJ, et al. Hyaluronic acid/PLGA core/shell fiber matrices loaded with EGCG beneficial to diabetic wound healing. *Adv Healthc Mater*. 2016;*5*(23):3035-3045.
49. Anagf V, Bhl M, He S. Advances in the management of skin wounds with synthetic dressings. *ClinMed Int Library*. 2016;*3*:1-6.
50. Li M, Chen J, Shi M, Zhang H, Ma PX, Guo B. Electroactive antioxidant polyurethane elastomers with shape memory property as non-adherent wound dressing to enhance wound healing. *Chem Eng J*. 2019;*375*:1999.
51. Kamocki K, Nör JE, Bottino MC. Effects of ciprofloxacin-containing antimicrobial scaffolds on dental pulp stem cell viability—in vitro studies. *Arch Oral Biol*. 2015;*60*(8):1131-1137.
52. Ma X, Xiao Y, Xu H, Lei K, Lang M. Preparation, degradation and in vitro release of ciprofloxacin-eluting ureteral stents for potential antibacterial application. *Mater Sci Eng C*. 2016;*66*:92-99.
53. Farsaei S, Khalili H, Farboud ES. Potential role of statins on wound healing: review of the literature. *Int Wound J*. 2012;*9*(3):238-247.
54. Perumal G, Pappuru S, Chakraborty D, Nandkumar AM, Chand DK, Doble M. Synthesis and characterization of curcumin loaded PLA—Hyperbranched polyglycerol electrospun blend for wound dressing applications. *Mater Sci Eng C*. 2017;*76*:1196-1204.
55. Kharazi AZ, Fathi MH, Bahmani F, Fanian H. Partially resorbable composite bone plate with controlled degradation rate, desired mechanical properties and bioactivity. *Polym Degrad Stab*. 2011;*96*(12):2055-2063.
56. Zhang J-F, Yang D-Z, Xu F, Zhang Z-P, Yin R-X, Nie J. Electrospun core– shell structure nanofibers from homogeneous solution of poly (ethylene oxide)/chitosan. *Macromolecules*. 2009;*42*(14):5278-5284.
57. Zhang Y, Huang Z-M, Xu X, Lim CT, Ramakrishna S. Preparation of core– shell structured PCL-r-gelatin bi-component nanofibers by coaxial electrospinning. *Chem Mater*. 2004;*16*(18):3406-3409.
58. Yang B-Y, Hu C-H, Huang W-C, Ho C-Y, Yao C-H, Huang C-H. Effects of bilayer nanofibrous scaffolds containing curcumin/lithospermi radix extract on wound healing in streptozotocin-induced diabetic rats. *Polymers*. 2019;*11*(11):1745.
59. do Rego ACM, Araújo Filho I, Damasceno BPGL, et al. Simvastatin improves the healing of infected skin wounds of rats. *Acta Cir Bras*. 2007;*22*:57-63.
60. Murphy CM, Haugh MG, O'brien FJ. The effect of mean pore size on cell attachment, proliferation and migration in collagen–glycosaminoglycan scaffolds for bone tissue engineering. *Biomaterials*. 2010;*31*(3):461-466.
61. Ho MH, Do TB-T, Dang NN-T, et al. Effects of an acetic acid and acetone mixture on the characteristics and scaffold–cell interaction of electrospun polycaprolactone membranes. *Appl Sci*. 2019;*9*(20):4350.
62. Sameh N, Aly UF, Abou-Taleb HA, Abdellatif AAH. Prospective role of simvastatin on wound healing: review of the literature. *J Bioequiv Bioavailab*. 2018;*10*(2):36-42.
63. Yen Y, Pu C, Liu C, et al. Curcumin accelerates cutaneous wound healing via multiple biological actions: the involvement of TNF-α, MMP-9, α-SMA, and collagen. *Int Wound J*. 2018;*15*(4):605-617.
64. Wang H-M, Chou Y-T, Wen Z-H, Wang Z-R, Chen C-H, Ho M-L. Novel biodegradable porous scaffold applied to skin regeneration. *PLoS One*. 2013;*8*(6):e56330.
65. Mun J, Kim Y, Kim B, Kim J, Kim M, Ko H. Simvastatin inhibits transforming growth factor-β1-induced expression of type I collagen, CTGF, and α-SMA in keloid fibroblasts. *Wound Repair Regen*. 2014;*22*(1):125-133.
66. Makpol S, Jam FA, Yusof YAM, Ngah WZW. Modulation of collagen synthesis and its gene expression in human skin fibroblasts by tocotrienol-rich fraction. *Arch Med Sci*. 2011;*7*(5):889-895.
67. Liu C, Zhu J, Hai B, et al. Single intraosseous injection of simvastatin promotes endothelial progenitor cell mobilization, neovascularization, and wound healing in diabetic rats. *Plast Reconstr Surg*. 2020;*145*(2):433-443.
68. Asai J, Takenaka H, Hirakawa S, et al. Topical simvastatin accelerates wound healing in diabetes by enhancing angiogenesis and lymphangiogenesis. *Am J Pathol*. 2012;*181*(6):2217-2224.
69. Ramhormozi P, Ansari JM, Simorgh S, et al. Simvastatin accelerates the healing process of burn wound in Wistar rats through Akt/mTOR signaling pathway. *Ann Anatomy-Anatomischer Anzeiger*. 2020;*236*:151652.
70. Ayati Najafabadi SA, Shirazaki P, Zargar Kharazi A, Varshosaz J, Tahriri M, Tayebi L. Evaluation of sustained ciprofloxacin release of biodegradable electrospun gelatin/poly (glycerol sebacate) mat membranes for wound dressing applications. *Asia-Pacif J Chem Eng*. 2018;*13*(6):e2255.

How to cite this article: Heydari, P., Zargar Kharazi, A., Asgary, S., & Parham, S. (2021). Comparing the wound healing effect of a controlled release wound dressing containing curcumin/ciprofloxacin and simvastatin/ciprofloxacin in a rat model: A preclinical study. *Journal of Biomedical Materials Research Part A*, 1–12. https://doi.org/10.1002/jbm.a.37292